

Martensitic Transformation and Superelastic Properties of Ti-Nb Base Alloys

Hee Young Kim* and Shuichi Miyazaki*

Division of Materials Science, University of Tsukuba, Tsukuba 305-8573, Japan

Ti-Nb base alloys have been proposed as prospective candidates for Ni-free biomedical superelastic alloys due to their excellent mechanical properties with good biocompatibility, and many kinds of Ti-Nb base alloys exhibiting shape memory effect or superelasticity have been developed up to now. However, typical Ti-Nb base superelastic alloys show a small recovery strain which is less than one third of the recovery strain of practical Ti-Ni superelastic alloys. Over the last decade there have been extensive efforts to improve the properties of Ti-Nb base superelastic alloys through microstructure control and alloying. Low temperature annealing and aging are very effective to increase the critical stress for slip due to fine subgrain structure and precipitation hardening. The addition of interstitial alloying elements such as O and N raises the critical stress for slip and improves superelastic properties. In this paper, the roles of alloying elements on the martensitic transformation temperature, crystal structure, microstructure and deformation behavior in the Ti-Nb base alloys are reviewed and the alloy design strategy for biomedical superelastic alloys is proposed. [doi:10.2320/matertrans.M2014454]

(Received December 16, 2014; Accepted February 23, 2015; Published April 25, 2015)

Keywords: *shape memory effect, superelasticity, martensitic transformation, titanium alloy, biomaterial, alloy design, microstructure control, crystal structure*

1. Introduction

Ti-Ni shape memory alloys have been used in a variety of industries because of their unique property of shape memory effect, which is an ability to remember their original shape and, after being deformed, recover the pre-deformed shape by heating.¹⁾ Couplings, fasteners, auto shut off valves, sensors and actuators are representative applications utilizing the shape memory effect.^{2,3)} Ti-Ni shape memory alloys also exhibit superelasticity, the unusual ability to undergo a large elastic deformation,^{4,5)} which makes them ideal to be used for cellular phone antennae, eyeglasses frames, orthodontic arch wires, guide wires and self-expanding stents.^{2,3,6)} Ti-Ni shape memory alloys have also been considered as attractive materials for biomedical implants.⁷⁻¹⁰⁾ However, there have been long-standing concerns regarding the risk of Ni allergy and hypersensitivity for long term use because of high amount of Ni content in Ti-Ni shape memory alloys.¹¹⁻¹⁴⁾ In order to reduce the potential risk of Ni, several surface modification techniques, such as oxidation, plasma spraying and chemical vapor deposition, have been proposed.¹⁵⁻²¹⁾ However, these methods do not guarantee absolute safety for long term use. The poor workability is another weakness of Ti-Ni shape memory alloys; only a shape of wire and tube is practically available.

β -type Ti-base alloys, which exhibit the reversible thermo-elastic martensitic transformation, have attracted much attention as candidates for biomedical shape memory alloys due to their attractive properties such as excellent biocompatibility, corrosion resistance and cold workability. The shape memory effect of Ti-base alloys was first reported in a Ti-35 mass%Nb alloy by Baker in 1971.²²⁾ The shape memory effect was also observed in Ti-10V-2Fe-3Al (1982)²³⁾ and Ti-Mo-Al alloys (1985).²⁴⁾ Since the early

2000s, there has been intensive research on the development of biomedical shape memory alloys consisting of only biocompatible or less toxic elements.²⁵⁻³³⁾ Particularly, there has been tremendous progress in developing Ti-Nb base shape memory alloys in the past decade and many Ti-Nb base alloys have been developed, e.g. Ti-Nb-Sn,^{26,34)} Ti-Nb-Al,^{31,32,35)} Ti-Nb-Ta,^{36,37)} Ti-Nb-Zr,³⁸⁻⁴⁴⁾ Ti-Nb-Mo,^{45,46)} Ti-Nb-Pd,⁴⁷⁾ Ti-Nb-O,⁴⁸⁾ Ti-Nb-N,^{49,50)} Ti-Nb-Pt,⁵¹⁾ Ti-Nb-Ta-Zr,⁵²⁻⁵⁴⁾ Ti-Nb-Zr-Sn,⁵⁵⁻⁵⁷⁾ Ti-Nb-Mo-Sn,⁵⁸⁻⁶⁰⁾ Ti-Zr-Nb-Sn,⁶¹⁾ Ti-Nb-Zr-Al⁶²⁾ and Ti-Nb-Zr-Mo-Sn.⁶³⁾

This paper aims to provide an overview of the recent works on Ti-Nb base shape memory alloys. Martensitic transformation characteristics and shape memory properties of Ti-Nb binary alloys are addressed in Section 2 and 3. The effect of substitutional alloying elements on superelastic properties of Ti-Nb base alloys is presented in Section 4. Section 5 is concerned with the effect of interstitial alloying elements on the microstructure and superelastic properties. The effect of omega phase on superelastic properties of Ti-Nb base alloys is discussed in Section 6. The effect of heat treatment condition on shape memory properties of Ti-Nb base alloys is briefly reviewed in Section 7. The alloy design strategy is proposed in Section 8. Finally, the conclusion gives a brief summary and includes future perspectives of Ti-base biomedical shape memory alloys.

2. Martensitic Transformation Characteristics of β -Ti Alloys

Pure Ti has a hexagonal close packed crystal structure (α phase) at room temperature. Upon heating Ti undergoes an allotropic phase transformation at 1159 K from the α phase to β phase with a body centered cubic crystal structure. Alloying elements alter the β transus temperature at which the alloy transforms completely to the β phase: α -stabilizers such as Al, Ga, Ge, O and N raise the β transus temperature while β -stabilizers such as Nb, Ta, Mo, V, Fe and Cr reduce

*Corresponding authors, E-mail: heeykim@ims.tsukuba.ac.jp, miyazaki@ims.tsukuba.ac.jp

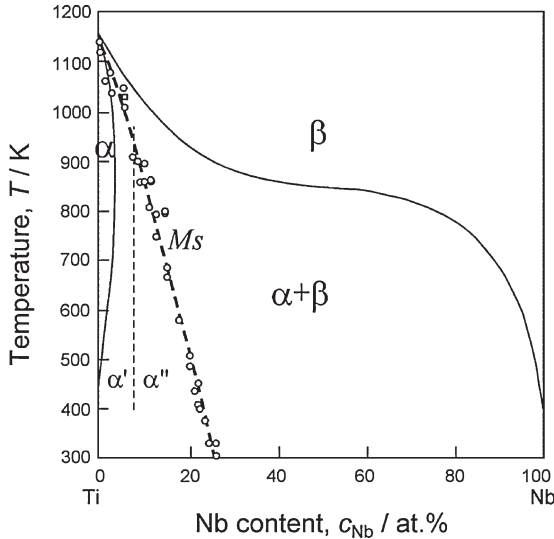


Fig. 1 Nb content dependence of M_s for Ti-Nb binary alloys.

the β transus temperature. It is considered that Sn and Zr behave neutrally, because they change the β transus temperature only slightly.

Ti alloys containing β -stabilizing alloying elements exhibit a martensitic transformation upon quenching from the β phase to hexagonal martensite (α') or orthorhombic martensite (α'') depending on the content of alloying elements, e.g., Nb.^{64–69)} The α' martensite is formed in relatively dilute alloys. The crystal structure of α' martensite is the same as that of α phase. The martensite structure changes to orthorhombic when the β -stabilizer content increases above a critical amount. The critical solute content for α'/α'' boundary depends on the solute elements. For example, the α' is formed with Mo content up to about 2 at% in Ti-Mo binary alloys, whereas the α' is formed with Nb content up to about 6 at% in Ti-Nb binary alloys.⁷⁰⁾ The α'/α'' boundary for Ti-Ta binary alloys is about 9 at% Ta.⁷⁰⁾ The martensitic transformation start temperature M_s decreases with increasing Nb content as shown in Fig. 1: M_s decreases by about 40 K with 1 at% increase of Nb content and M_s becomes lower than room temperature when the Nb content increases more than 25.5 at%.^{71,72)} It is noted that the critical content shows a scatter in literatures due to different quenching rate and impurity level.⁷¹⁾

The orthorhombic martensite (α'') will be considered in detail in this paper, because shape memory effect (SME) and superelasticity (SE) in Ti-base alloys are associated with the reversible transformation between the β (bcc) phase and α'' (orthorhombic) phases. The martensitic transformation start temperature (M_s) decreases with increasing β -stabilizer content. It should be noted that a meta-stable omega (ω) phase forms at low temperatures. Recently, crystallographic characteristics of α'' martensite, such as internal structure, self-accommodation morphologies and interfacial structure, in Ti-Nb base alloys, were systematically investigated.^{73–77)} It was confirmed that the crystallography of the α'' martensite is well explained by the phenomenological theory of martensite crystallography (PTMC)^{78–80)} and topological model.⁸¹⁾

The shape memory effect and superelasticity are due to the reversible and thermoelastic phase transformation. Shape

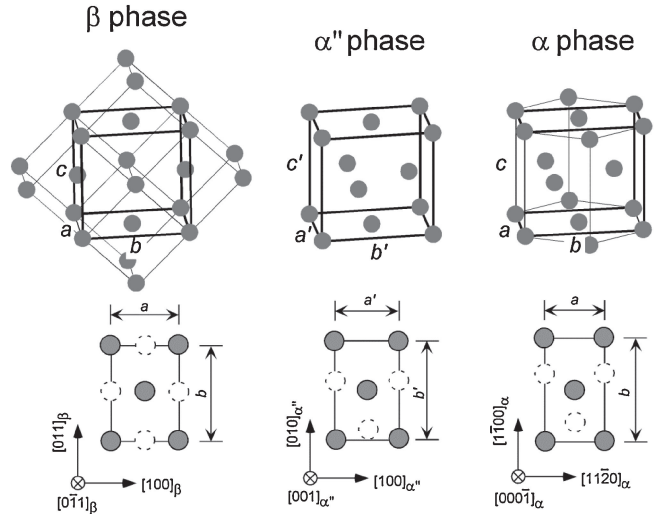


Fig. 2 Crystal structures of β , α'' and α phases and their lattice correspondences.

memory properties, such as temperature hysteresis, cyclic stability, transformation strain, are affected by the geometric compatibilities between parent and martensite phases, i.e. the lattice correspondence between martensite and parent phases and their lattice constants. Particularly, the transformation strain is directly governed by the lattice constants of martensite and parent phases. Thus, in order to develop shape memory alloys with a larger recovery strain, it is indispensable to investigate the composition dependence of lattice constants of both phases as well as transformation temperatures.

Figure 2 shows a schematic illustration exhibiting the crystal structures of the β , α'' and α phases and their lattice correspondences.⁸²⁾ It has been confirmed that lattice constants of α'' phase change with β -stabilizer content and considered that the α'' orthorhombic martensite is an intermediate structure between the body centered cubic structure of β phase and hexagonal structure of α -Ti. The lattice constants a' and c' in the orthorhombic cell (α'' phase) correspond to the lattice constants a and c in the hexagonal cell (α phase), which also correspond to a_0 and $\sqrt{2}a_0$ in the body centered cubic cell where a_0 is the lattice constant of β phase. The lattice constant b' in the orthorhombic cell corresponds to $\sqrt{3}a$ in the hexagonal cell as well as $\sqrt{2}a_0$ in the body centered cubic cell as shown in Fig. 2. Figure 3 shows the Nb content dependence of b'/a' and c'/a' ratios of α'' martensite in Ti-Nb binary alloys.⁸²⁾ It is seen that both of b'/a' and c'/a' decrease from the values of α -Ti to the values of β phase with increasing Nb content, implying that the α'' martensite is a comprise phase between α' and β phases.²³⁾ The values of $b/a(= 1.732)$ and $c/a(= 1.586)$ of α -Ti and those ($= 1.414$) of the β phase are indicated by dashed lines. Similar composition dependence of α'' lattice constants has been reported in Ti-Ta alloys.⁸³⁾ For the Ti-Nb binary alloys, the lower compositional limit of α'' -orthorhombic martensite phase is 6 at% Nb as mentioned above, while the upper compositional limit of α'' -orthorhombic martensite phase is estimated to be 32 at% Nb by a linear extrapolation. The lattice deformation strains, η_1 , η_2 and η_3 , needed to form the α'' phase from the β phase along three principal axes also

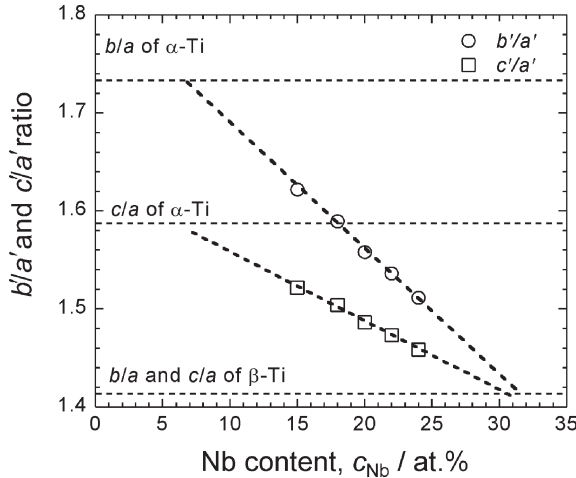


Fig. 3 Nb dependence of b'/a' and c'/a' of the α'' -orthorhombic martensite phase.

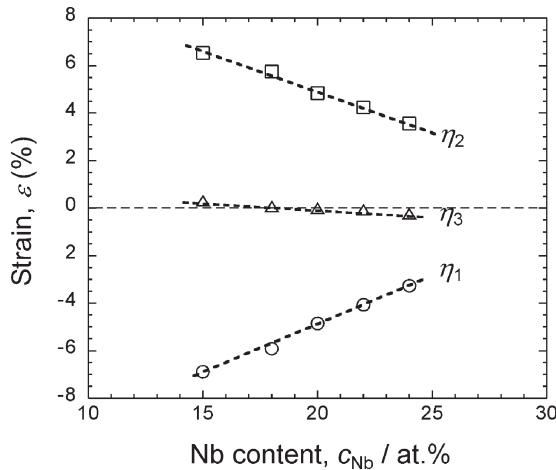


Fig. 4 Lattice deformation strains needed to form the α'' phase from the β phase along three principal axes.

change with β -stabilizer content as shown in Fig. 4.⁷¹⁾ The lattice deformation strains are given as:

$$\eta_1 = \frac{a' - a_0}{a_0}, \quad \eta_2 = \frac{b' - \sqrt{2}a_0}{\sqrt{2}a_0}, \quad \eta_3 = \frac{c' - \sqrt{2}a_0}{\sqrt{2}a_0}$$

where a' , b' and c' are the lattice constants of α'' martensite and a_0 is that of β phase. As shown in Fig. 4, two principal lattice strains (η_1 and η_2) of the martensitic transformation are approximately equal and opposite in sign, and their absolute values decrease with increasing Nb content.⁷¹⁾ Lattice strain η_3 is small compared with η_1 and η_2 , ranging from -0.24 to 0.30%. It is noted that η_3 becomes zero when Nb content is about 20 at%. A small amount of η_3 implies that lattice invariant shear (LIS) is not necessary for martensitic transformation. For Ti-Ta binary alloys, η_3 is zero when Ta content is 21 at%.⁸³⁾ For Ti-xNb-3Al alloys, η_3 is zero at $x = 23$ at%.⁷³⁾ It has been confirmed that non-twinned martensites are formed when η_3 is small in Ti-Nb, Ti-xNb-3Al and Ti-Ta alloys.

Habit planes of non-twinned martensites are close to $(hk\bar{k})$, where $h > k$, e.g. $(544)_\beta$ in Ti-21 at% Ta,⁸³⁾ $(755)_\beta$ in Ti-(16-23)Nb-3Al (at%)⁷³⁾ and $(755)_\beta$ in Ti-20Nb.⁷⁴⁾ It should be

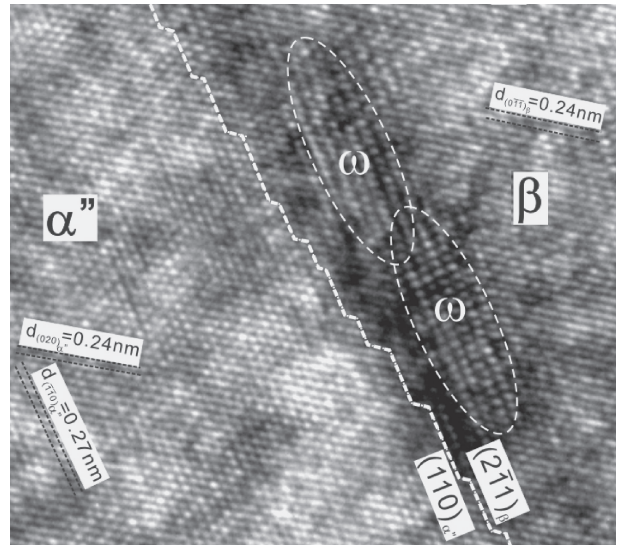


Fig. 5 A high resolution transmission electron micrograph showing the β/α'' interface in a Ti-24Nb alloy.

noted that martensites with internal twin of $\{111\}$ type I is formed when β -stabilizer content is small. It was also found that the β/α'' interfaces (habit planes) in Ti-Nb alloys exhibit a terraces/steps structure as shown in Fig. 5,⁷⁴⁾ where the terrace planes are parallel to $(2\bar{1}\bar{1})_\beta/(110)_{\alpha''}$. The terraces/steps structure is considered as a typical relaxed structure of an irrational interface. No misfit dislocation was observed along the interface, indicating the terrace planes are coherent.

3. Shape Memory Effect and Superelasticity in Ti-Nb Binary Alloys

Shape memory effect and superelasticity have been confirmed in many Ti-Nb base alloys including Ti-Nb binary alloys.^{22,30,71,84)} For the Ti-Nb binary system, Ti-(26-27) at% Nb alloys exhibit superelasticity at room temperature while shape memory effect is observed in Ti-(20-25) at% Nb alloys as shown in Fig. 6. The maximum recovery strain of 3% was obtained at about 5% tensile strain in solution treated Ti-(25-27) at% Nb alloys.³⁰⁾ The small recovery strain in Ti-Nb alloys is due to the small transformation strain as well as the low critical stress for slip.

The strain induced by the martensitic transformation shows strong orientation dependence. The transformation strain produced by the lattice distortion due to the martensitic transformation in a single crystal can be calculated using the lattice constants of the parent β phase (a_0) and the orthorhombic α'' martensite phase (a' , b' and c'). Figure 7 shows the Nb content dependence of transformation strains for three representative orientations, [011], [001] and $[\bar{1}11]$ of the β phase.⁸²⁾ The insert in Fig. 7 exhibits a [001] – [011] – $[\bar{1}11]$ standard stereographic triangle showing a schematic orientation dependence of the transformation strain expressed by contour lines. It is seen that the largest transformation strain is obtained along the [011] direction of the β phase, which corresponds to the [010] direction of the α'' phase. The orientation dependence of the transformation strain was experimentally confirmed in Ti-22Nb-6Ta³⁶⁾ and Ti-24Nb-3Al³²⁾ alloys.

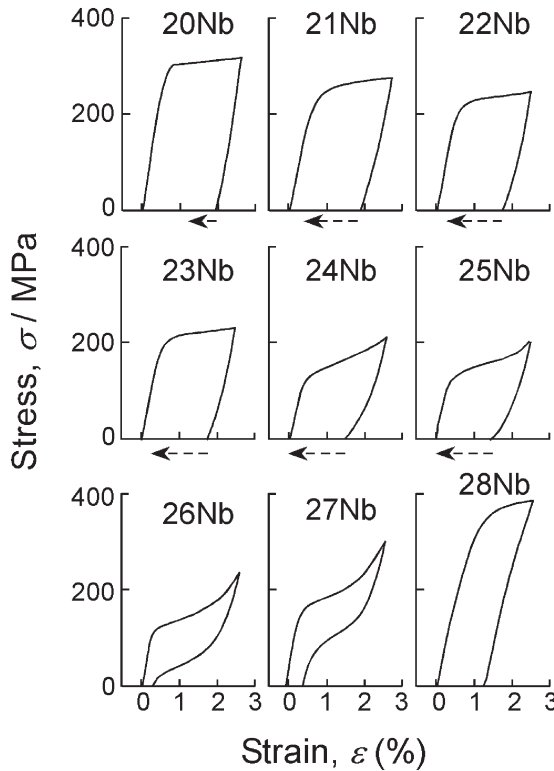


Fig. 6 Stress-strain curves of Ti-(20-28)Nb alloys.

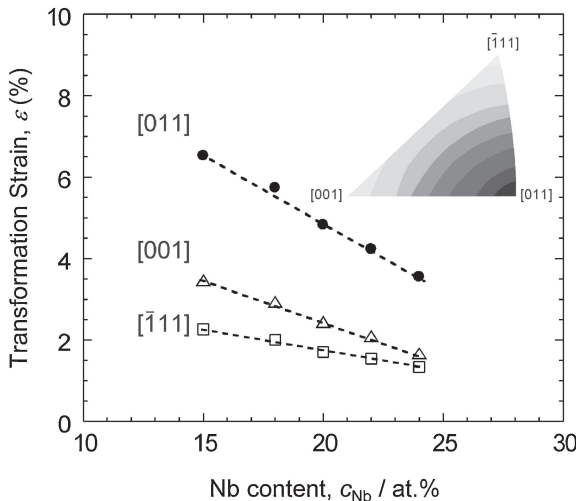


Fig. 7 Nb content dependence of the transformation strain for Ti-Nb binary alloys and orientation dependence of the transformation strain.

It is seen that the transformation strains along the three direction decrease with increasing Nb content. It has been reported that a strong deformation texture of $\{100\}\langle 110 \rangle$ is developed in severely cold-rolled β -Ti alloys. On the other hand, a strong recrystallization texture of $\{112\}\langle 110 \rangle$ is developed by solution treatment, indicating that the maximum transformation strain can be obtained along the rolling direction for both deformation and recrystallization textures. It is noted that the transformation strain along the [011] direction, i.e. the largest transformation strain, of the Ti-27 at% Nb alloy which shows superelastic behavior at room temperature is only 2.5%. This value is much smaller than that for the B2-B19' transformation in Ti-Ni alloys. In order

to increase the transformation strain, the Nb content should be reduced, but the decrease in Nb content raises the transformation temperature as shown in Fig. 1 and causes not to reveal superelasticity at room temperature. This intrinsic small transformation strain is one of drawbacks of Ti-Nb superelastic alloys.

4. Effect of Substitutional Alloying Elements

In order to improve superelastic properties, the addition of ternary elements has been considered. The quantitative information on the transformation temperature is essential to develop shape memory alloys. However, there have been limited researches to date on the effect alloying elements on the martensitic transformation temperature of β -Ti alloys. This is because of difficulties in measuring transformation temperatures by differential scanning calorimetry (DSC) measurements due to the small enthalpy of β - α'' transformation and the formation of thermal and/or athermal ω phase.

Additions of all alloying elements regardless of β -stabilizer or α -stabilizer decrease M_s of Ti-Nb based alloys in literatures which have been published to date. M_s decreases by about 30 K or 35 K with 1 at% increase of Ta or Zr content in the Ti-22Nb alloy, respectively.⁸⁵⁾ It is noted that Zr lowers M_s although it has been considered as a neutral element for α/β transformation temperature. The addition of Sn, which is also considered as a neutral element, considerably decreases the transformation temperature: M_s and A_f (reverse transformation finish temperature) decrease by 150 K with increasing Sn content from 4 to 5 at% in Ti-16Nb-Sn alloys.²⁶⁾ A similar decreasing effect of Sn on the martensitic transformation temperature was also observed in Ti-Nb-Zr-Sn quaternary alloy⁵⁵⁾ although the effect in decreasing the transformation temperature was relatively small compared with Ti-Nb-Sn ternary alloys. Addition of noble alloying elements such as Pt, Au and Pd also decreases transformation temperature of Ti-Nb base alloys.⁴⁷⁻⁵¹⁾ For example, M_s decreases by about 160 K with an increase of 1 at% Pt.⁵¹⁾ The addition of Mo also decreases the martensitic transformation temperatures. Yazan *et al.*⁴⁵⁾ reported that Ti-27Nb, Ti-24Nb-1Mo, Ti-21Nb-2Mo and Ti-18Nb-3Mo alloys exhibit stable superelasticity at RT, indicating that the addition of 1 at% Mo decreases M_s by 120 K. The reduction of M_s by Cu addition in Ti-Nb base alloys was reported to be 100 K/at%Cu.⁸⁶⁾ Other 3-d transition metal elements such as Fe, Cr, Co and Ni were also reported to decrease the transformation temperature of Ti-Nb base alloys although no quantitative measurements were provided.⁸⁷⁾ It is also noted that an addition of Al decreases M_s with a slope of 40 K/at%Al even though Al is considered as an α -stabilizer.^{31,73)} Other α -stabilizers such as Ga and Ge also decrease transformation temperature of Ti-Nb base alloys.⁸⁸⁾

Figure 8 shows cyclic stress-strain curves of Ti-27Nb, Ti-22Nb-7Ta, Ti-22Nb-6Zr, Ti-21Nb-2Mo and Ti-19Nb-2Pt alloys obtained at room temperature.⁸²⁾ All the alloys have similar martensitic transformation temperature and exhibit superelasticity. The maximum recovery strain ε_r , which is the sum of elastic strain ε_e and superelastic transformation strain ε_{se} , was observed 2.0% in the Ti-27Nb alloy. The Ti-22Nb-

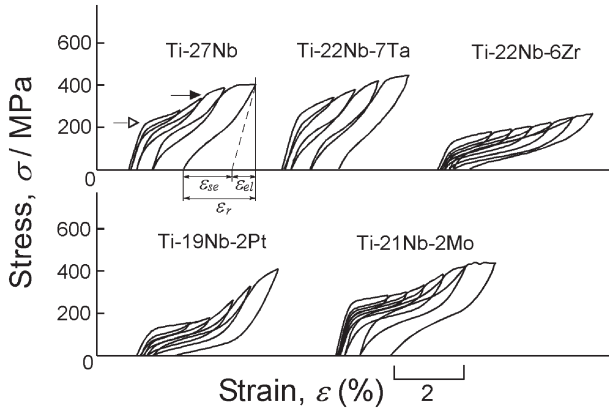


Fig. 8 Stress-strain curves obtained by strain increment cyclic loading and unloading tensile tests in Ti-Nb base alloys.

6Zr, Ti-19Nb-2Pt and Ti-21Nb-2Mo alloys reveal good superelasticity with a larger recovery strain when compared with the Ti-27Nb alloy. The maximum recovery strains of 3.5%, 3.0% and 3.2% were obtained in the Ti-22Nb-6Zr, Ti-19Nb-2Pt and Ti-21Nb-2Mo alloys, respectively. This is due to the fact that the addition of Zr, Pt or Mo as a substitute of Nb is effective to increase the transformation strain along the [011] direction with keeping M_s similar. As mentioned above, not only transformation temperature but also transformation strain decreases with increasing the amount of alloying elements. For the Ti-Nb binary alloys, the transformation strain decreased by about 0.34% with 1 at% increase of Nb content, while the transformation strain decreases by 0.13% with 1 at% increase of Zr content. On the other hand, M_s decreases by about 40 K or 35 K with 1 at% increase of Nb or Zr content in the Ti-22Nb alloy, respectively. This indicates that the addition of Zr as a substitute of Nb, with keeping M_s similar, is effective to increase the transformation strain. The addition of Pt as a substitute of Nb is also effective to increase the transformation strain, because Pt is four times more effective in reducing M_s of Ti-Nb alloys than Nb, while it is only three times more effective in decreasing transformation strain than Nb. On the other hand, the addition of Ta is not effective to increase the transformation strain because of its weak impact in decreasing M_s .⁸⁹⁾ The addition of Mo was also found to increase the transformation strain and improve the superelastic properties through the systematic investigation of the effect of Mo and Nb concentration in Ti-Nb-Mo alloys.⁴⁵⁾ However, the increase of Mo at the expense of Nb in the condition of revealing superelasticity at room temperature causes the formation of both thermal and athermal ω phases.⁴⁶⁾

5. Effect of Interstitial Alloying Elements

Interstitial alloying elements such as O and N significantly suppress the martensitic transformation of Ti-Nb alloys. For Ti- x Nb-1O alloys, superelasticity is observed when x is 22 at%,⁴⁸⁾ implying that the addition of 1 at% O to Ti-Nb alloys decreases M_s by about 160–200 K because the effect of 1 at% O in decreasing the martensitic transformation temperature is equivalent to that of 4–5 at%Nb. N shows a similar effect on the martensitic transformation temperature; the

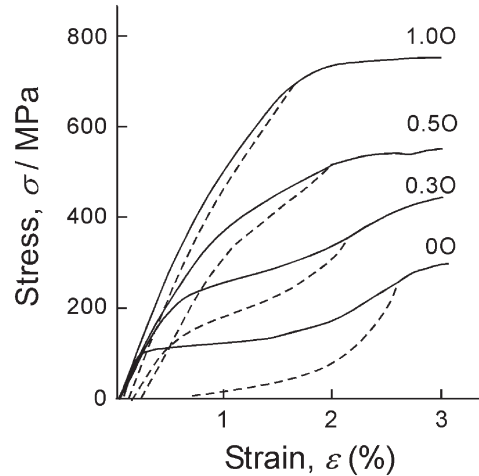


Fig. 9 Effect of oxygen addition on the stress-strain curve of a Ti-26Nb alloy.

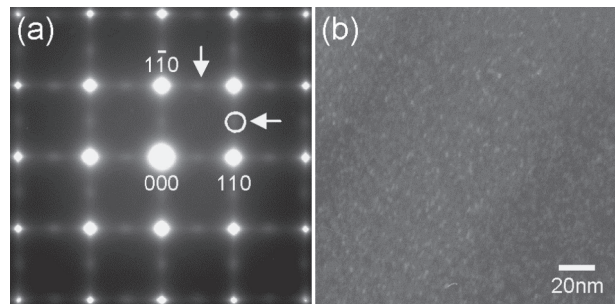


Fig. 10 (a) A selected area diffraction pattern and (b) a dark field micrograph of a Ti-26Nb-1O alloy obtained from the [001] zone axis.

addition of 1 at% N to Ti-Nb⁴⁹⁾ and Ti-Nb-4Zr-2Ta⁹⁰⁾ alloys decreases M_s by about 200 K. However, the martensitic transformation temperature decreases by 75 K with 1 at% increase of N content for the Ti-18Zr-13Nb alloy.⁹¹⁾ It is suggested that this weaker effect of N on the martensitic transformation temperature in the alloy with relatively a higher content of Zr is due to its larger lattice parameter. On the other hand, C and B exhibit little effect on the transformation temperature due to its limited solubility in β Ti-Nb alloys.^{92,93)}

The addition of interstitial alloying elements is very effective in increasing the stress for plastic deformation. Figure 9 shows stress-strain curves of Ti-26Nb-O alloys obtained at room temperature.⁹⁴⁾ It is clearly seen that not only the first yielding stress but also the secondary yielding stress increases with increasing oxygen content, where the first yielding corresponds to stress induced martensitic transformation and the second yielding is due to the plastic deformation. Similar effects were also reported in a Ti-24Nb-4Zr-8Sn alloy.⁹⁵⁾ It is also interesting to note that the Ti-26Nb-1O alloy shows non-linear elastic behavior with a large recovery strain. It has been proposed that the suppression of martensitic transformation and non-linear elastic behavior are due to the formation of nano-sized lattice modulation (nano-domain) induced by interstitial oxygen atoms.⁹⁶⁾

Figure 10(a) shows a selected area diffraction pattern of the Ti-26Nb-1O alloy obtained from the [001] zone axis.⁹⁶⁾

Diffuse streaks along $\langle 110 \rangle$ directions and the intensity maxima at $\{h + \frac{1}{2}k + \frac{1}{2}l\}$ positions are seen between primary diffraction spots of the β phase. It has been confirmed that the diffuse streaks are due to the $\{\bar{1}\bar{1}0\}\langle 110 \rangle$ type transverse displacement.⁹⁷⁾ The nano-domains are clearly visible in the dark-field micrograph obtained from the intensity maxima ($\frac{3}{2}\frac{1}{2}0$) as shown in Fig. 10(b). The nano-domain structure is caused by randomly distributed oxygen atoms. As shown in Fig. 11,⁹⁴⁾ strain fields are formed around oxygen atoms in octahedral sites: there are three types of octahedral sites which oxygen atoms can occupy in the β phase. For example, an atom which occupies the site A induces a local strain field with a direction of [001]. The local strain field can be relaxed by shuffling of atoms on adjacent $(0\bar{1}1)$ planes in the [011] and [011̄] directions, which is crystallographically same as the shuffling mode of the martensitic transformation from β phase to α'' phase as shown in Fig. 2. This implies that the oxygen atom facilitates the martensitic transformation locally. The stress fields induced by the oxygen atoms in other octahedral sites can be relaxed by the different shuffling modes. It has been confirmed that there are six variants of nano-domains, which are corresponding to six shuffling modes of the β to α'' martensitic transformation.⁹⁷⁾ The six nano-domain variants are introduced equivalently since the oxygen atoms distribute randomly and evenly when no stress is applied. Nano-domain variants act as local barriers against the growth of other nano-domain variants. As a result, it is concluded that the interstitial alloying elements suppress a long range martensitic transformation due to the presence of multiple nano-domain variants although they enhance the martensitic transformation locally. It has been reported that several unique properties, such as a larger elastic strain, invar-like behavior, non-linear elastic behavior and abnormal temperature dependence of shape memory behavior, observed in β -Ti alloys containing a larger amount of interstitial alloying elements, are successfully explained by the presence of a nano-domain structure.⁹⁷⁻¹⁰⁰⁾

Figure 12 shows the change in X-ray diffraction (XRD) profiles with strain during tensile deformation for the Ti-26Nb and Ti-26Nb-O alloys.⁹⁸⁾ In the XRD profiles of the Ti-26Nb alloy, a reflection peak from martensite phase appeared at $\varepsilon = 0.3\%$ where apparent yielding occurred, and the peak increased with increasing applied strain, indicating that the stress induced martensitic transformation occurs upon loading. On the other hand, the XRD profiles of the Ti-26Nb-O alloy reveal no distinct peaks from martensite phase upon loading until $\varepsilon = 2.5\%$, whereas a reflection peak from the β phase shifted continuously to a higher 2θ angle and became broader with increasing tensile strain, suggesting that second-order-like transformation occurred. This can also be explained by the nano-domain structure: the stress induced martensitic transformation was suppressed by the local barriers of the randomly distributed nanodomain variants.

The addition of interstitial alloying elements is effective for improving cyclic stability of superelastic properties. Figure 13 shows the comparison of stability of superelastic properties of Ti-26Nb and Ti-23Nb-1N alloys during cyclic deformation.⁴⁹⁾ The tensile stress was applied until the strain reached 2.5%, and then the stress was removed. The loading-unloading tensile test was repeated until 500th cycle as shown in Fig. 13. For the Ti-26Nb alloy, the critical stress for inducing martensitic transformation and superelastic strain decreased, while irrecoverable residual strain increased. Only 1.2% of superelastic strain was obtained at the 500th cycle in the Ti-26Nb alloy. The increase in the residual strain during the cyclic deformation is mainly due to the increase in the residual martensite which is stabilized by plastic deformation. On the other hand, it is clearly seen that stable cyclic deformation behavior was observed in the Ti-23Nb-1N when

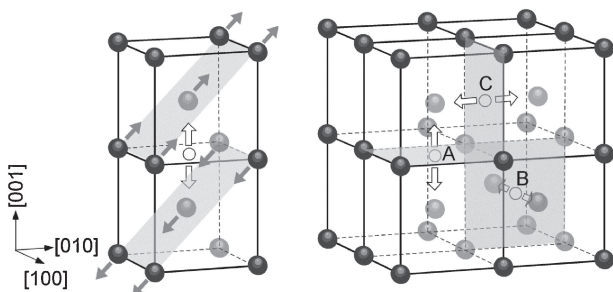


Fig. 11 Schematic illustration of three types of octahedral sites in a bcc lattice and the stress relaxation by shuffling of atoms.

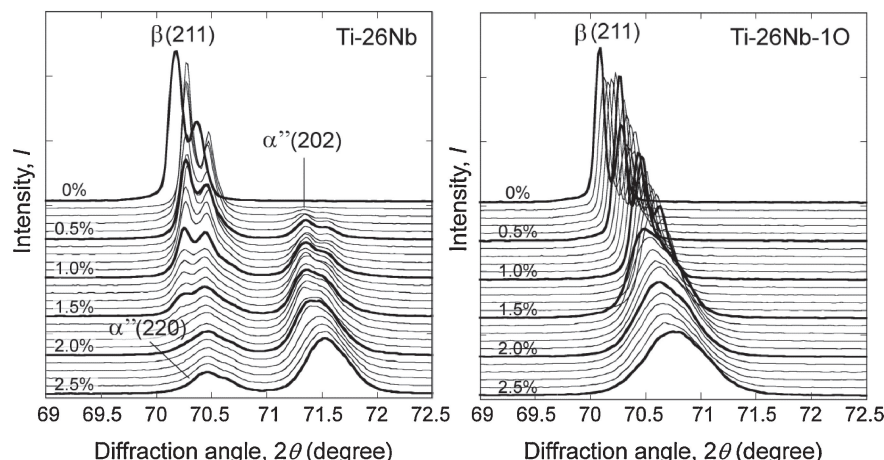


Fig. 12 XRD profiles obtained by *in-situ* measurements for Ti-26Nb and Ti-26Nb-1O alloys.

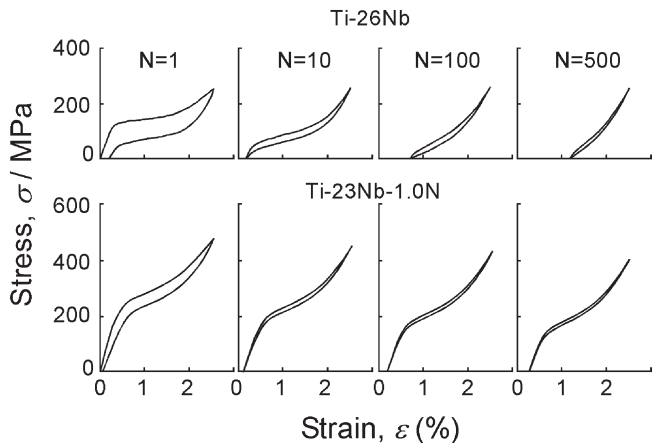


Fig. 13 Comparison of cyclic deformation behavior of Ti-26Nb and Ti-23Nb-1.0N alloys.

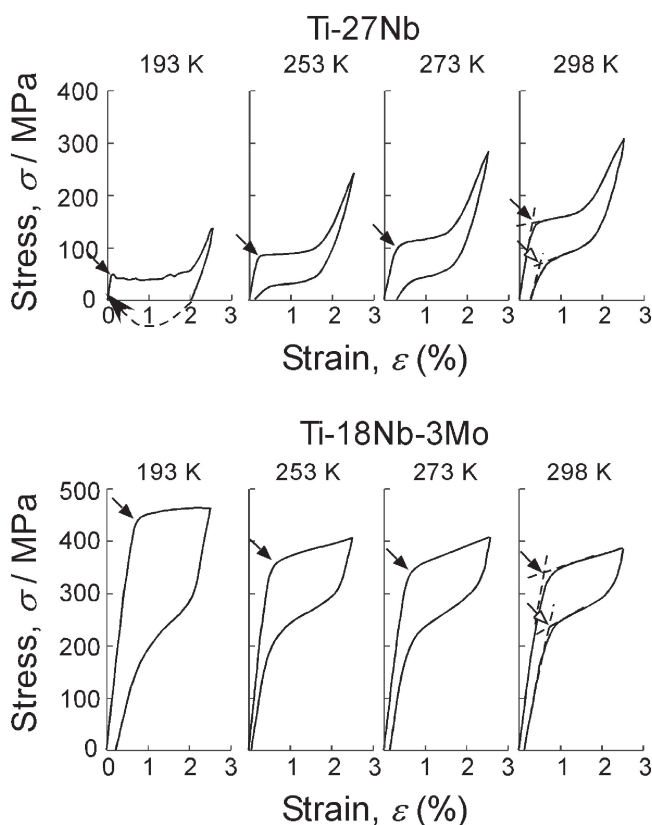


Fig. 14 Effect of test temperature on superelastic behavior of Ti-27Nb and Ti-18Nb-3Mo alloys.

compared with the Ti-26Nb alloy; superelastic strain was slightly decreased during the cyclic deformation and 2.2% of superelastic strain was obtained even at the 500th cycle. This is due to the increase in the critical stress for slip by the solid solution strengthening effect of N.

6. Effect of Athermal Omega Phase

As mentioned above, in order to increase the transformation strain the amount of β -stabilizing alloying elements should be reduced. However, this leads to increased formation of athermal ω phase. The athermal ω phase has

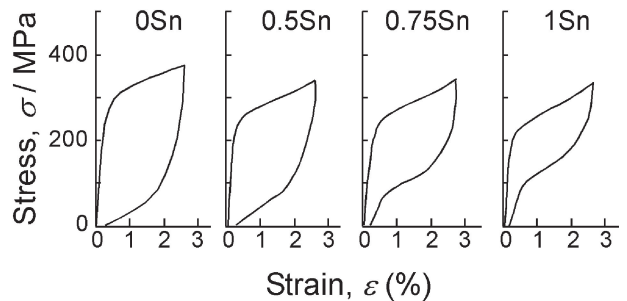


Fig. 15 Effect of Sn content on superelastic behavior of Ti-15Nb-3Mo-(0-1)Sn alloys.

received great attentions due to its pronounced effect on mechanical and electrical properties. The athermal ω phase also affects superelastic properties of β -Ti alloys. Figure 14 shows stress-strain curves obtained at various temperatures for Ti-27Nb and Ti-18Nb-3Mo alloys.⁴⁶⁾ For the Ti-27Nb alloy, the apparent yield stress indicated by a solid-headed arrow, which is corresponding to the critical stress for inducing martensitic transformation, decreases with decreasing test temperature since the martensite phase becomes more stable as temperature decreases. On the other hand, the Ti-18Nb-3Mo alloy exhibits the opposite temperature dependence of the critical stress for inducing martensitic transformation. This is due to a strong tendency of the Ti-18Nb-3Mo alloy to form athermal ω phase upon cooling. Furthermore, the athermal ω phase increases the stress hysteresis and deteriorates superelastic properties. It has been reported that Al and Sn are effective in suppressing the formation of ω phase.^{58,59,101)} Figure 15 shows the effect of Sn addition on the loading-unloading stress-strain curve of the Ti-15Nb-3Mo alloy.⁵⁸⁾ It is clearly seen that stress hysteresis decreases with increasing Sn content. The suppression of the athermal ω phase also leads to an improvement of superelastic recovery strain owing to the reduced stress for martensitic transformation.

7. Thermomechanical Treatment

A higher critical stress for slip deformation is an important factor for stabilizing and enhancing superelastic properties. It has been generally acknowledged that the following methods are effective in increasing the critical stress for plastic deformation: (1) solid solution hardening, (2) precipitation hardening, (3) work hardening and (4) grain size refinement. As mentioned above, the addition of interstitial alloying elements such as O and N increases the critical stress for slip significantly due to the solution hardening effect. The latter three methods for increasing the critical stress for slip can be achieved by thermo-mechanical treatment. Annealing at a temperature below the recrystallization temperature after severe cold working increases the critical stress for plastic deformation due to work hardening and grain size refinement, resulting in the improvement of superelastic properties.^{39,71)} Aging at a temperature between 473 and 673 K is also effective to increase the critical stress for slip and stabilize superelasticity owing to the formation of isothermal ω phase.^{72,102)}

Table 1 Effects of alloying element on M_s and transformation strain along the [011] direction in Ti-Nb binary and Ti-Nb-X ternary alloys.

Alloying element	Effect in changing M_s temperature (K/at%)	Effect in changing transformation strain (%/at%)	Alloy composition showing superelasticity at RT	
Nb	-40	-0.34	Ti-(26,27)Nb	Ref. 71)
Ta	-30	-0.28	Ti-22Nb-(6,7)Ta	Ref. 37), 85)
Mo	-120	-0.89	Ti-24Nb-1Mo, Ti-21Nb-2Mo, Ti-18Nb-3Mo	Ref. 45)
Pt	-160	-0.95	Ti-19Nb-2Pt	Ref. 51)
Cu	-100		Ti-18Nb-4Cu	Ref. 86)
Zr	-35	-0.13	Ti-22Nb-6Zr, Ti-15Nb-18Zr	Ref. 85), 91)
Sn	-150		Ti-16Nb-4.9Sn	Ref. 26)
Al	-40	-0.27	Ti-24Nb-3Al	Ref. 31), 73)
O	-160~200		Ti-(22,23)Nb-1O	Ref. 48), 97)
N	-200		Ti-(22~24)Nb-1N	Ref. 49), 90)

8. Alloy Design Strategy

A small transformation strain at compositions showing superelastic behavior is one of the major drawbacks of Ti-Nb binary alloys. Thus the addition of alloying elements is crucial to improve superelastic properties because the crystal structure of martensite phase can be modified by the addition of alloying elements. Alloy composition affects both martensitic transformation temperature and transformation strain; therefore we need to consider the effect of composition on martensitic transformation temperature and crystal structure quantitatively. The effects of alloying element on M_s and transformation strain along the [011] direction in Ti-Nb binary and Ti-Nb-X ternary alloys are summarized in Table 1. Among many alloying elements investigated up to date, Zr is the most effective in increasing the transformation strain. The increase in Zr content in Ti-Nb-Zr alloys exhibits weak effect on the transformation strain while the transformation temperature decreases with increasing Zr content at a similar level as that of Nb. Therefore, the addition of Zr as a substitute of Nb, while keeping the martensitic transformation temperature the same, increases the transformation strain. Furthermore, Zr is considered as a highly biocompatible alloying element.¹⁰³⁾ The addition of Mo in replacement of Nb is also effective to increase transformation strain with keeping the transformation temperature similar. However, the decrease in the amount of β stabilizing alloying elements accelerates the formation of the ω phase. The addition of Sn is effective to suppress the formation of ω phase and improves the superelastic properties. In conclusion, it is proposed that Ti-Zr-Nb-Sn alloy system is one of the promising materials for practical biomedical superelastic alloys. Very recently, it was reported that a remarkably large recovery strain of around 7%, which is comparable to conventional Ti-Ni base superelastic alloys, is achieved in a Ti-24Zr-10Nb-2Sn alloy as shown in Fig. 16⁶¹⁾ by the combination of beneficial effects of Zr and Sn. The addition of interstitial alloying elements such as O and N has two beneficial effects on the superelastic properties. Firstly, O and N reduce the transformation temperature remarkably, resulting in that the superelasticity can be obtained at lower Nb compositions which lead to a larger transformation strain.

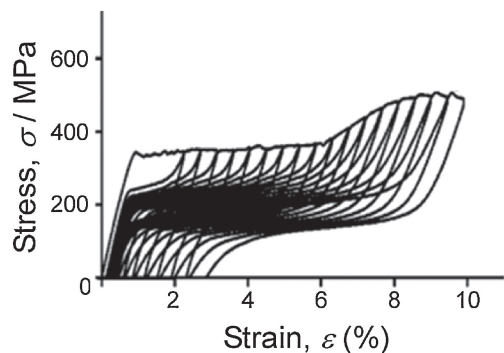


Fig. 16 Stress-strain curves obtained by strain increment cyclic loading and unloading tensile tests in a Ti-24Zr-10Nb-2Sn alloy.

Secondly, O and N increase the critical stress for slip due to the solution hardening effect. As a result, it is suggested that Ti-Zr-Nb-(Sn) base alloys with small amount of interstitial elements can be good candidates for biomedical superelastic alloys.

9. Concluding Remarks

Over the last decade there have been impressive progresses in understanding the basic characteristics of the martensitic transformation of β -Ti alloys and many shape memory alloys have been developed. Recent researches show that the intrinsic problem of small transformation strain and low strength of Ti-Nb base alloys can be overcome by the addition of alloying elements and microstructure control. Through the optimization of composition and thermomechanical treatment, the superelastic properties of β -Ti alloys can be further improved. It is confidently expected that β -Ti superelastic alloys will further expand the applications of shape memory alloys in biomedical field.

Acknowledgments

This work was partially supported by JSPS KAKENHI Grant Number 26249104 and MEXT KAKENHI Grant Number 25102704.

REFERENCES

- 1) S. Miyazaki and K. Otsuka: *ISIJ Int.* **29** (1989) 353–377.
- 2) Y. Yamauchi, I. Ohkata, K. Tsuchiya and S. Miyazaki: *Shape Memory and Superelastic Alloys*, (Woodhead Publishing, Cambridge, 2011).
- 3) K. Otsuka and C. M. Wayman: *Shape Memory Materials*, (Cambridge University Press, Cambridge, 1998).
- 4) S. Miyazaki, T. Imai, Y. Igo and K. Otsuka: *Met. Trans. A* **17** (1986) 115–120.
- 5) S. Miyazaki and K. Otsuka: *Met. Trans. A* **17** (1986) 53–63.
- 6) T. Yoneyama and S. Miyazaki: *Shape Memory Alloys for Biomedical Applications*, (Woodhead Publishing, Cambridge, 2009).
- 7) M. S. Moneim, K. Firoozbakhsh, A. A. Mustapha, K. Larsen and M. Shahinpoor: *Clin. Orthop.* **402** (2002) 251–259.
- 8) S. Kujala, A. Pajala, M. Kallioinen, A. Pramila, J. Tuukkanen and J. Ryhanen: *Biomater.* **25** (2004) 353–358.
- 9) M. H. Elahinia, M. Hashemi, M. Tabesh and S. B. Bhaduri: *Prog. Mater. Sci.* **57** (2012) 911–946.
- 10) R. R. Adharapurapu and K. S. Vecchio: *Exper. Mech.* **47** (2007) 365–371.
- 11) E. Denkhaus and K. Salnikow: *Crit. Rev. Oncol. Hematol.* **42** (2002) 35–56.
- 12) M. Es-Souni, M. Es-Souni and H. F. Brandies: *Anal. Bioanal. Chem.* **381** (2005) 557–567.
- 13) W. Haider, N. Munroe, C. Pulletkurthi, P. K. S. Gill and S. Amruthaluri: *J. Mater. Eng. Perform.* **18** (2009) 760–764.
- 14) Q. Li, Y. Zeng and X. Tang: *Australas. Phys. Eng. Sci. Med.* **33** (2010) 129–136.
- 15) A. Michiardi, C. Aparicio, J. A. Planell and F. J. Gil: *J. Biomed. Mater. Res.* **77B** (2006) 249–256.
- 16) Y. Cheng, W. Cai, H. T. Li and Y. F. Zheng: *J. Mater. Sci.* **41** (2006) 4961–4964.
- 17) R. Singh and N. B. Dahotre: *J. Mater. Sci.* **18** (2007) 725–751.
- 18) M. Barrabes, A. Michiardi, C. Aparicio, P. Sevilla, J. A. Planell and F. J. Gil: *J. Mater. Sci.* **18** (2007) 2123–2129.
- 19) W. Chrzanowski, E. A. A. Neel, D. A. Armitage and J. C. Knowles: *J. Mater. Sci.* **19** (2008) 1553–1557.
- 20) C. L. Chu, C. Guo, X. B. Sheng, Y. S. Dong, P. H. Lin, K. W. K. Yeung and P. K. Chu: *Acta Biomater.* **5** (2009) 2238–2245.
- 21) E. Espinar, J. M. Llamas, A. Michiardi, M. P. Ginebra and F. J. Gil: *J. Mater. Sci.* **22** (2011) 1119–1125.
- 22) C. Baker: *Metal Sci. J.* **5** (1971) 92–100.
- 23) T. W. Duerig, J. Albrecht, D. Richter and P. Fischer: *Acta Metall.* **30** (1982) 2161–2172.
- 24) H. Sasano and T. Suzuki: Proc. 5th Int. Conf. on Titanium, (Frankfurt, Deutsche Gesellschaft fur Metallkunde, 1985) pp. 1667–1674.
- 25) T. Grosdidier and M. J. Philippe: *Mater. Sci. Eng. A* **291** (2000) 218–223.
- 26) E. Takahashi, T. Sakurai, S. Watanabe, N. Masahashi and S. Hanada: *Mater. Trans.* **43** (2002) 2978–2983.
- 27) H. Hosoda, Y. Fukui, T. Inamura, K. Wakashima, S. Miyazaki and K. Inoue: *Mater. Sci. Forum* **426–432** (2003) 3121–3126.
- 28) H. Y. Kim, Y. Ohmatsu, J. I. Kim, H. Hosoda and S. Miyazaki: *Mater. Trans.* **45** (2004) 1090–1095.
- 29) T. Maeshima and M. Nishida: *Mater. Trans.* **45** (2004) 1096–1100.
- 30) H. Y. Kim, H. Satoru, J. I. Kim, H. Hosoda and S. Miyazaki: *Mater. Trans.* **45** (2004) 2443–2448.
- 31) Y. Fukui, T. Inamura, H. Hosoda, K. Wakashima and S. Miyazaki: *Mater. Trans.* **45** (2004) 1077–1082.
- 32) T. Inamura, Y. Fukui, H. Hosoda, K. Wakashima and S. Miyazaki: *Mater. Trans.* **45** (2004) 1083–1089.
- 33) T. Zhou, M. Aindow, S. P. Alpay, M. J. Blackburn and M. H. Wu: *Scr. Mater.* **50** (2004) 343–348.
- 34) F. Nozoe, H. Matsumoto, T. K. Jung, S. Watanabe, T. Saburi and S. Hanada: *Mater. Trans.* **48** (2007) 3007–3013.
- 35) M. U. Farooq, F. A. Khalid, H. Zaigham and I. H. Abidi: *Mater. Lett.* **121** (2014) 58–61.
- 36) H. Y. Kim, T. Sasaki, K. Okutsu, J. I. Kim, T. Inamura, H. Hosoda and S. Miyazaki: *Acta Mater.* **54** (2006) 423–433.
- 37) H. Y. Kim, S. Hashimoto, J. I. Kim, T. Inamura, H. Hosoda and S. Miyazaki: *Mater. Sci. Eng. A* **417** (2006) 120–128.
- 38) J. I. Kim, H. Y. Kim, T. Inamura, H. Hosoda and S. Miyazaki: *Mater. Sci. Eng. A* **403** (2005) 334–339.
- 39) J. I. Kim, H. Y. Kim, T. Inamura, H. Hosoda and S. Miyazaki: *Mater. Trans.* **47** (2006) 505–512.
- 40) F. Sun, Y. L. Hao, S. Nowak, T. Gloriant, P. Laheurte and F. Prima: *Mech. Behav. Biomed. Mater.* **4** (2011) 1864–1872.
- 41) J. Y. Zhang, F. Sun, Y. L. Hao, N. Gazdecki, E. Leburn, P. Vermaut, R. Portier, T. Gloriant, P. Laheurte and F. Prima: *Mater. Sci. Eng. A* **563** (2013) 78–85.
- 42) Y. Cui, Y. Li, K. Luo and H. Xu: *Mater. Sci. Eng. A* **527** (2010) 652–656.
- 43) Q. Li, M. Niinomi, M. Nakai, Z. Cui, S. Zhu and X. Yang: *Mater. Sci. Eng. A* **536** (2012) 197–206.
- 44) L. W. Ma, H. S. Cheng and C. Y. Chung: *Intermetallics* **32** (2013) 44–50.
- 45) Y. Al-Zain, H. Y. Kim, H. Hosoda, T. H. Nam and S. Miyazaki: *Acta Mater.* **58** (2010) 4212–4223.
- 46) Y. Al-Zain, H. Y. Kim, T. Koyano, H. Hosoda, T. H. Nam and S. Miyazaki: *Acta Mater.* **59** (2011) 1464–1473.
- 47) D. H. Ping, Y. Mitarai and F. X. Yin: *Scr. Mater.* **52** (2005) 1287–1291.
- 48) J. I. Kim, H. Y. Kim, H. Hosoda and S. Miyazaki: *Mater. Trans.* **46** (2005) 852–857.
- 49) M. Tahara, H. Y. Kim, H. Hosoda and S. Miyazaki: *Func. Mater. Lett.* **02** (2009) 79–82.
- 50) A. Ramarolahy, P. Castany, F. Prima, P. Laheurte, I. Péron and T. Gloriant: *J. Mech. Behav. Biomed. Mater.* **9** (2012) 83–90.
- 51) H. Y. Kim, N. Oshika, J. I. Kim, T. Inamura, H. Hosoda and S. Miyazaki: *Mater. Trans.* **48** (2007) 400–406.
- 52) N. Sakaguchi, M. Niinomi, T. Akahori, J. Takeda and H. Toda: *Mater. Sci. Eng. C* **25** (2005) 363–369.
- 53) M. Niinomi, T. Akahori and M. Nakai: *Mater. Sci. Eng. C* **28** (2008) 406–413.
- 54) Y. F. Zhu, L. Q. Wang, M. M. Wang, Z. T. Liu, J. N. Qin, D. Zhang and W. J. Lu: *J. Mech. Behav. Biomed. Mater.* **12** (2012) 151–159.
- 55) Y. L. Hao, S. J. Li, S. Y. Sun and R. Yang: *Mater. Sci. Eng. A* **441** (2006) 112–118.
- 56) F. Sun, Y. L. Hao, J. Y. Zhang and F. Prima: *Mater. Sci. Eng. A* **528** (2011) 7811–7815.
- 57) Y. Yang, P. Castany, M. Cornet, I. Thibon, F. Prima and T. Gloriant: *J. Alloy. Compd.* **591** (2014) 85–90.
- 58) M. F. Ijaz, H. Y. Kim, H. Hosoda and S. Miyazaki: *Scr. Mater.* **72–73** (2014) 29–32.
- 59) Y. Al-Zain, Y. Sato, H. Y. Kim, H. Hosoda, T. H. Nam and S. Miyazaki: *Acta Mater.* **60** (2012) 2437–2447.
- 60) D. C. Zhang, Y. F. Mao, M. Yan, J. J. Li, E. L. Su, Y. L. Li, S. W. Tan and J. G. Lin: *J. Mech. Behav. Biomed. Mater.* **20** (2013) 29–35.
- 61) L. L. Pavón, H. Y. Kim, H. Hosoda and S. Miyazaki: *Scr. Mater.* **95** (2015) 46–49.
- 62) H. Tada, T. Yamamoto, X. Wang and H. Kato: *Mater. Trans.* **53** (2012) 1981–1985.
- 63) D. Kent, G. Wang, Z. Yu and M. S. Dargusch: *Mater. Sci. Eng. A* **527** (2010) 2246–2252.
- 64) D. L. Moffat and D. C. Larbalestier: *Metall. Trans. A* **19** (1988) 1677–1686.
- 65) J. P. Morniroli and M. Gantois: *Mem. Sci. Rev. Metall.* **70** (1973) 831–842.
- 66) C. Baker and J. Sutton: *Philos. Mag.* **19** (1969) 1223–1255.
- 67) K. S. Jepson, A. R. G. Brown and J. A. Gray: *The Science, Technology and Application of Titanium*, ed. by R. I. Jafee and N. Promisel, (Pergamon Press, London, 1970) p. 677.
- 68) T. Ahmed and H. J. Rack: *J. Mater. Sci.* **31** (1996) 4267–4276.
- 69) J. C. Williams: Proc. Second Int. Conf. on Titanium, (New York, USA, Plenum Press, 1973) p. 1433.
- 70) E. W. Collings: *Materials Properties Handbook: Titanium Alloys*, (ASM, Materials Park, USA, 1994).
- 71) H. Y. Kim, Y. Ikebara, J. I. Kim, H. Hosoda and S. Miyazaki: *Acta Mater.* **54** (2006) 2419–2429.
- 72) H. Y. Kim, J. I. Kim, T. Inamura, H. Hosoda and S. Miyazaki: *Mater. Sci. Eng.* **438–440** (2006) 839–843.

- 73) T. Inamura, J. I. Kim, H. Y. Kim, H. Hosoda, K. Wakashima and S. Miyazaki: *Philos. Mag.* **87** (2007) 3325–3350.
- 74) Y. W. Chai, H. Y. Kim, H. Hosoda and S. Miyazaki: *Acta Mater.* **56** (2008) 3088–3097.
- 75) Y. W. Chai, H. Y. Kim, H. Hosoda and S. Miyazaki: *Acta Mater.* **57** (2009) 4054–4064.
- 76) T. Inamura, H. Y. Kim, H. Hosoda and S. Miyazaki: *Philos. Mag.* **90** (2010) 3475–3498.
- 77) T. Inamura, H. Hosoda and S. Miyazaki: *Philos. Mag.* **93** (2013) 618–634.
- 78) J. S. Bowles and J. K. Mackenzie: *Acta Metall.* **2** (1954) 129–137.
- 79) J. K. Mackenzie and J. S. Bowles: *Acta Metall.* **2** (1954) 138–147.
- 80) M. S. Wechsler, D. S. Lieberman and T. A. Read: *Trans. AIME* **197** (1953) 1503–1515.
- 81) R. C. Pond and S. Celotto: *Int. Mater. Rev.* **48** (2003) 225–245.
- 82) S. Miyazaki and H. Y. Kim: *Mater. Sci. Forum* **561–565** (2007) 5–21.
- 83) K. A. Bywater and J. W. Christian: *Philos. Mag.* **25** (1972) 1249–1273.
- 84) H. Y. Kim, J. I. Kim, T. Inamura, H. Hosoda and S. Miyazaki: *Mater. Sci. Eng. A* **438–440** (2006) 839–843.
- 85) S. Miyazaki, H. Y. Kim and H. Hosoda: *Mater. Sci. Eng. A* **438–440** (2006) 18–24.
- 86) Y. Horiuchi, K. Nakayama, T. Inamura, H. Y. Kim, K. Wakashima, S. Miyazaki and H. Hosoda: *Mater. Trans.* **48** (2007) 414–421.
- 87) Y. Horiuchi, T. Inamura, H. Y. Kim, K. Wakashima, S. Miyazaki and H. Hosoda: *Mater. Trans.* **47** (2006) 1209–1213.
- 88) T. Inamura, Y. Fukui, H. Hosoda, K. Wakashima and S. Miyazaki: *Mater. Sci. Eng. C* **25** (2005) 426–432.
- 89) P. J. S. Buenconsejo, H. Y. Kim, H. Hosoda and S. Miyazaki: *Acta Mater. Sci. Eng. A* **57** (2009) 1068–1077.
- 90) M. Tahara, H. Y. Kim, H. Hosoda, T. H. Nam and S. Miyazaki: *Mater. Sci. Eng. A* **527** (2010) 6844–6852.
- 91) M. Tahara, H. Y. Kim, T. Inamura, H. Hosoda and S. Miyazaki: *Mater. Trans.* **50** (2009) 2726–2730.
- 92) Y. Horiuchi, T. Inamura, H. Y. Kim, K. Wakashima, S. Miyazaki and H. Hosoda: *Mater. Trans.* **48** (2007) 407–413.
- 93) H. Hosoda, Y. Horiuchi, T. Inamura, K. Wakashima, H. Y. Kim and S. Miyazaki: *Mater. Sci. Forum* **638–642** (2006) 2046–2051.
- 94) H. Y. Kim: *Mater. Japan* **53** (2014) 11–17.
- 95) E. G. Obbard, Y. L. Hao, R. J. Talling, S. J. Li, Y. W. Zhang, D. Dye and R. Yang: *Acta Mater.* **59** (2011) 112–125.
- 96) Y. Nii, T. Arima, H. Y. Kim and S. Miyazaki: *Phys. Rev. B* **82** (2010) 214104.
- 97) M. Tahara, H. Y. Kim, T. Inamura, H. Hosoda and S. Miyazaki: *Acta Mater.* **59** (2011) 6208–6218.
- 98) M. Tahara, H. Y. Kim, T. Inamura, H. Hosoda and S. Miyazaki: *J. Alloy. Compd.* **577** (2013) S404–S407.
- 99) H. Y. Kim, L. Wei, S. Kobayashi, M. Tahara and S. Miyazaki: *Acta Mater.* **61** (2013) 4874–4886.
- 100) M. Tahara, H. Y. Kim, T. Inamura, H. Hosoda and S. Miyazaki: *Acta Mater.* **80** (2014) 317–326.
- 101) P. J. S. Buenconsejo, H. Y. Kim and S. Miyazaki: *Acta Mater.* **57** (2009) 2509–2515.
- 102) M. Tahara, H. Y. Kim, T. Inamura, H. Hosoda and S. Miyazaki: *Acta Mater.* **57** (2009) 2461–2469.
- 103) A. Biesiekierski, J. Wang, M. A. H. Gepreel and C. Wen: *Acta Biomater.* **8** (2012) 1661–1669.